DOI:10.11916/j.issn.1005-9113.18022

Review: Coincidence Momentum Imaging: Principle and Application in Molecular Reaction Dynamics

Li Zhang[1*] *and Huailiang Xu*[2**]

(*1.Communications and Electronic Information Department, Shanghai Vocational College of Science and Technology, Shanghai 201800, China; 2.State Key Laboratory of Integrated Optoelectronics, College of Electronic Science and Engineering, Jilin University, Changchun 130012, China*)

Abstract: Coincidence Momentum Imaging (CMI) is a powerful imaging technique that can determine the full momentum vectors of all particles released from a single parent molecule in coincidence and thus provide detailed information on transient molecular structures. So far, the CMI technique has been extensively employed for investigating a variety of molecular reaction dynamics induced, e.g., by particle collisions, intense laser fields and synchrotron radiation. In this article, we first introduce the principle of the CMI technique, which is followed by several typical experimental designs of the CMI systems realizing the coincidence momentum detections. We then present representative examples of studying molecular reaction dynamics using the CMI technique.

Keywords: Coincidence momentum imaging; Intense laser fields; Molecular reaction dynamics

CLC number: O561.4 **Document code**: A **Article ID**: 1005-9113(2018)04-0001-14

1 Introduction

The Coincidence Momentum Imaging (CMI) technique[1], with which the full three-dimensional (3D) momentum vectors of electrons and/or ions ejected from an ionizing or a fragmenting molecule can be measured, has been an extensively employed imaging tool for studying various molecular reaction dynamics over the last 20 years[2-5]. For example, by utilizing its unique properties including high momentum resolution, large solid angle collection, and coincidence measurement, the CMI technique has been successfully employed to gain detailed insight into the molecular fragmentation channels[6], infer electronic structure of molecules from the emission patterns of electrons[7], identify the ionization pathways[8] and so forth. Moreover, with this technique, molecular reaction dynamics in various experimental conditions such as intense femtosecond[9] and attosecond[10] light fields, charged particle impact[11-12], synchrotron radiation[13-14], and free electron lasers[15] can be studied. This gives rise to tremendous progress in the development of the CMI technique and consequently a variety of the CMI systems have been designed, e.g., with different spectrometers[2-5,16-18], detectors[19-33] and other devices[34-47] in order to increase count rate and detection efficiency, improve multi-hit capability, discriminate false coincidence events and thermal momentum uncertainty, obtain better resolution, and minimize the effect of the extraction field in electron- or ion-impact schemes etc.

In this paper, we will review recent progress in the CMI technique. We begin with a brief introduction to the basic principle of the momentum coincidence measurement, based on which different CMI systems have been designed. We will then present an overview of recent advance in the CMI systems designed, e.g., with different spectrometers, detectors and gas-jet targets. Finally, we will give several representative examples of investigating molecular reaction dynamics

Received 2018-02-24.

Sponsored by the National Natural Science Foundation of China (Grant Nos.61625501 and 61427816), Open Fund of the State Key Laboratory of High Field Laser Physics (SIOM), and Fundamental Research Funds for the Central Universities.

* Corresponding author. E-mail: zhangli19833@126.com;

** Corresponding author. Winner of the National Science Fund for Distinguished Young Scholars, and Winner of the Program for New Century Excellent Talents in University of Ministry of Education. E-mail: huailiang@jlu.edu.cn.

using the CMI technique.

2 Principle of the CMI Technique

In this section, take the typical CMI apparatus shown in Fig.1 for instance, we will briefly introduce the principle of the CMI technique that enables the 3D momentum measurements of photon-electron and photon-ion in coincidence. The CMI apparatus in Fig.1 is assumed to be in a high vacuum chamber with a background pressure up to the regime of 10^{-10}–10^{-11} mbar, and it is composed of a molecular beam, a laser beam interacting with the molecular beam in the interaction area, a spectrometer equipped with a set of electrodes producing a weak homogeneous electrostatic field and a set of coils producing a weak homogeneous magnetic field, and two multi-hit time- and position-sensitive detectors equipped respectively at the two ends of the spectrometer.

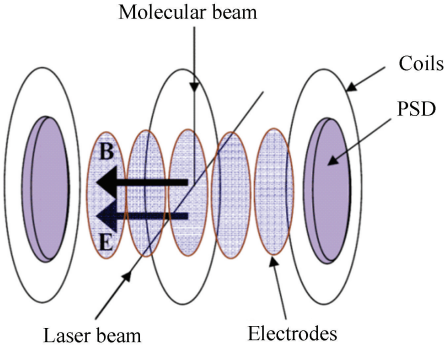

Fig. 1 A typical CMI apparatus for photon-electron and photon-ion detection (PSD: position-sensitive detector) [48]

In the CMI measurement with a laser as the excitation source, the laser beam is usually crossed with the molecular beam at right angles to induce various molecular reactions such as ionization, dissociation and fragmentation. The polarization direction of the laser beam is set parallel to the detection plane. The density of the molecular beam is controlled to make the number of ionized molecules per laser pulse less than one unity. The spectrometer in the CMI technique is used to extract and guide generated ions and electrons from the interaction region towards the two multi-hit time- and position-sensitive detectors by the weak homogeneous electrostatic field generated from the electrodes when a suitable voltage is applied on. A weak homogeneous magnetic field can also be produced in parallel to the electrostatic field by several separate coils with proper currents applied on them, in order to confine the resultant electrons and ions in the spectrometer. Both the fields are perpendicular to the molecular beam direction and the laser propagation direction. The fields are chosen such that a solid angle of detection of up to 4π can be achieved for the electrons and ions at the same time.

The multi-hit time- and position-sensitive detectors are applied to obtain each particle's 3D momentum information by recording its two-dimensional (2D) position (x,y) where the particle hits the detector, and its arrival time t at the detector.

The time and position information data can be written event by event into a list mode file (LMF) for further online/offline data analysis. The measured flight time and position for each particle in an event can be transformed to reconstruct the 3D momentum components in any desired coordinate frame. For example, supposing the Cartesian lab-coordinate system is desired, one can define the system as following: the molecular beam propagation direction, the laser beam propagation direction and the electrostatic field are along the x, y and z axis, respectively. The three momentum components of the ith ion gained from the laser molecular interaction, $p^i = (p_x^i, p_y^i, p_z^i)$, in the laboratory frame can be expressed as

$$p_x^i = m_i \Delta x/t \tag{1}$$

$$p_y^i = m_i \Delta y/t \tag{2}$$

$$p_z^i = m_i l_a/t - (1/2) q_i E_s t \tag{3}$$

where q_i and m_i are the charge and mass of the ith ion respectively, and Δx, Δy are the displacements of the ion from the position where the ion with $p_x = p_y = 0$ would hit, t is the time-of-flight of the ion from the reaction volume to the detector, l_a is the travelling distance of the ion in the z-axis direction, and E_s is the magnitude of the homogenous electrostatic field of the spectrometer.

The three momentum components of the electron gained from the laser molecular interaction, $p^e = (p_x^e, p_y^e, p_z^e)$, in the laboratory frame can be expressed as

$$p_x^e = \{eB/[2\sin(\alpha/2)]\}[-x\cdot\cos(\alpha/2) + y\cdot\sin(\alpha/2)] \tag{4}$$

$$p_y^e = \{eB/[2\sin(\alpha/2)]\}[x\cdot\sin(\alpha/2) + y\cdot\cos(\alpha/2)] \tag{5}$$

$$p_z^e = m_e l_a/t - (1/2) e E_s t \tag{6}$$

where m_e and e are the mass and the charge of the electron respectively, B is the magnitude of the

homogenous magnetic field, and α depends on the ratio of the time-of-flight t to the electron orbital period T_0 with the following relation

$$\alpha = mod(t, T_0) \times 360° \quad (7)$$

where $T_0 = 2\pi m_e / eB$. For details of expressions of the full 3D momentum vectors for both ions and electrons in the CMI technique, the readers are referred to Ref.[3].

Under the momentum conservation condition, a particular ionization or fragmentation pathway of molecules from one particular charge state of interest can be uniquely identified by selecting sets of particles whose sum-momentum P_s fulfills $|P_s| = 0$. As a result, false coincidence events resulting from multiple parent molecules in the reaction zone can be removed.

3 Recent Progress of the CMI Technique

Because of the superiority of the CMI technique for investigating molecular reaction dynamics, much effort has been made so far to improve its performance, such as enhancing the resolution of CMI detection in time, position, momentum, angular, and energy domains, increasing count rate and detection efficiency, improving multi-hit capability, discriminating false coincidence events and thermal momentum uncertainty, eliminating the effect of extraction field in electron- or ion-impact schemes and so on. In this section, we will give an overview of typical experimental CMI systems with different spectrometers, detectors, gas-jet targets, electron- and ion-impact designs.

3.1 Spectrometer in CMI Systems

The most often employed spectrometers in the CMI technique are the so-called "Reaction Microscopy" spectrometers. The Reaction Microscopy spectrometer has two types of electric field designs, i.e., cold target recoil ion momentum spectroscopy (COLTRIMS)[2-4], and velocity mapping coincidence imaging (VMI)[1,5]. The COLTRIMS spectrometer adopts a combination of a weak homogeneous electrostatic field and a weak homogeneous magnetic field, as shown in Fig.1. The use of the homogeneous magnetic field is to confine the electron trajectories, enabling electrons to arrive on the detector because the electrons usually are more energetic than the ions. Therefore, the trajectory of electrons in 3D space is spiral shaped between the reaction region and the detector plane. It is the shape of "spiral" that extends the detection solid angles of 4π to higher electron energies and unlimited length of the spectrometer for electrons as well. Meanwhile the magnetic field has only tiny influence on ions' trajectories due to the large mass of ions.

On the other hand, the VMI spectrometer utilizes an inhomogeneous electric field to realize 3D velocity focusing. In this scheme, a three-electrode electrostatic lens composed of three equally spaced parallel plate electrodes is adopted, in which the three electrodes are defined as repeller, accelerator and ground, as shown in Fig.2[1]. Particles produced in the reaction region are first pushed away by the repeller plate, and then accelerated after passing the accelerator plate toward the open ground electrode. Afterwards the particles enter a time-of-flight tube between the ground electrode and a time- and position-sensitive detector, which is a vacuum enclosure usually referred to field-free drift region. After passing through the tube, the charged particles are detected by the time and position sensitive detector. All particles that have the same initial velocity vector can be mapped on the detector at the same position, thus compensating for their initial position of creation. The VMI spectrometer simultaneously achieves time and position focusing.

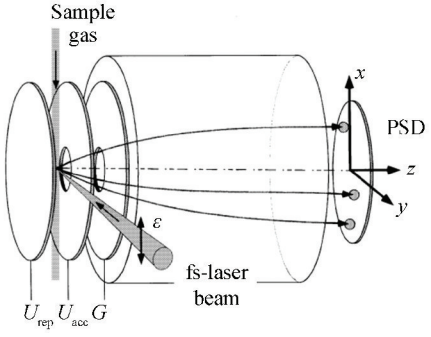

Fig.2 The VMI spectrometer produced by a three-electrode electrostatic lens (rep: repeller electrode; acc: accelerator electrode; *G*: ground electrode)[1]

In addition to the three ring electrodes in the above VMI spectrometer, a fourth additional ring electrode was also applied on the other side of the reaction area for simultaneously realizing both the position and time focusing effects[16]. This discriminates false coincidence events from the coincidence data and enables determining with a high resolution the momenta of fragment ions. The discrimination of the false coincidence events also

helps obtain the yields of different fragmentation channels with less uncertainties.

The spectrometer that employed both transverse and longitudinal electric fields for the CMI system was also developed to investigate the decomposition of CD^+ ions induced by strong ultrafast laser pulses[17]. This spectrometer allowed high-resolution separation of all decomposition pathways and the measurement of nearly zero kinetic energy release, for a parent molecule with notable mass asymmetry at the expense of double measurement time.

Another spectrometer for the CMI technique using SIMION was designed recently[18]. This spectrometer can simulate both the ion and electron trajectories. Different from the COLTRIMS and VMI spectrometers, on the ion side of the spectrometer a stronger electric field, a longer region with homogeneous electric field, and an electrostatic lens are used. In front of the ion detector an extra field-free drift region is applied. This field design remarkably improves the determination of fragmentation channel of methyloxirane[18]. On the electron side of the spectrometer, only a homogenous electric field was employed, which enables a 4π solid angle collection of electrons that could have a kinetic energy of up to 35 eV. This indicates that this spectrometer does not require a magnetic field to confine the electron trajectories. However, the shortcoming of the spectrometer configuration is that the speed of the time-of-flight of the electrons is reduced.

3.2 Detector in CMI Systems

The CMI systems equipped with different kinds of 3D detectors were designed, which consist of microchannel plate (MCP) detectors with fast delay-line anode readouts[19], cross wire detectors[20], wedge-strip detectors[21-22], dual-CCD detectors[23], multi-pixel semiconductor detectors[24-26], fast-frame complementary metal-oxide semiconductors (CMOS) camera[27,28] and so force. Here we will briefly introduce two types of detectors, i.e., the MCP detectors with delay-line anodes and the fast-frame CMOS camera. For the information on other detectors, the readers can refer to Refs. [20-26].

The MCP detector with fast delay-line anode readouts is the most widely used one in the CMI measurements. A pair of MCPs are used for registration of recoil ions and electrons via amplifying the collected signal. A MCP is a thin fabricate plate which includes millions of thin and conductive glass channels, each of which serves as an independent secondary electron multiplier. Secondary electrons are then accelerated by a high electric field. Afterwards the delay-line anodes are used for the MCPs'2D position readout with high resolution. The delay line anode is composed of a wire array and an anode holder. The wire array includes two pairs of delay-line helical propagation lines which are wound around a supporting holder. Each twisted pair consists of a signal wire and a reference wire and is responsible for one dimension. The detected particle position for each dimension is encoded independently by the difference of the signal arrival times at both ends for each parallel pair delay-line of the signal wire. The sum of these arrival times for each pair is a constant for each particle due to the constant length of each wire. The delay-line anode and its variations[29-31] have enjoyed a huge popularity as a result of the small dead time, high count rate, as well as high temporal and spatial resolution. Recently the delay-line anode has been developed from dual-layer to three-layer[32-33]. A fast hexanode style delay-line detector, described in Fig.3, with enhanced multi-hit capability has been realized, which can reduce multi-hit dead times down to 5 ns[33].

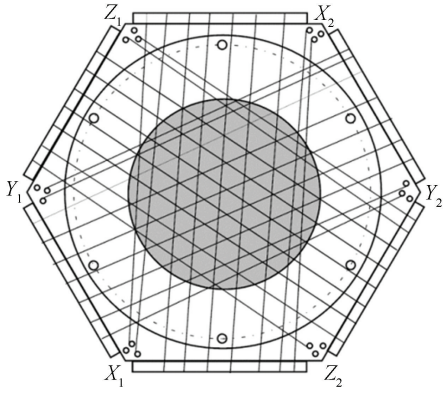

Fig.3 Sketch of the hexanode[33]

Recently, the fast frame CMOS camera was presented as a detection system of the CMI technique[27]. In this detection system, a conventional MCP/phosphor screen ion imager and a fast frame CMOS camera were used for obtaining the ion positions through real-time centroiding, meanwhile a single anode photomultiplier tube (PMT) and a high-speed digitizer were employed for gaining the time-of-flight spectrum of ions. The multi-hit capability of this system is realized by the correlations of ion spot intensity with the corresponding peaks of the time-of-flight spectrum, which has been demonstrated

successfully for methyl iodide[27].

3.3 Gas-jet Target in CMI Systems

Normally the CMI technique requires the gas-jet target at very low temperatures, since at room temperature the momentum measurement of recoil ions would be very insensitive to the scattering process because of the thermal momentum spreading. Pre-cooling of the gas-jet target can slow down the gas-jet velocity in order to lower the initial target momentum.

In the VMI technique, the gas-jet target is normally not pre-cooled. The sample gas can be sent into the sample vacuum chamber by a variable leak valve through a micro-syringe and then skimmed by a skimmer (with a typical diameter of ~500 μm) to form an effusive molecular beam in an ultrahigh vacuum chamber. The spectrometer design with the three ring electrodes in this technique can realize a high spatial resolution.

In the COLTRIMS technique, benefiting from the design of a supersonic gas-jet, the gas sample is pre-cooled in order to lower the thermal spreading, resulting in a higher resolution[3-4]. The well localized internally cold gas-jet target is generated by supersonic expansion of the gas sample through a small nozzle with a typical diameter of ~10 μm. A skimmer with a typical diameter of ~100 μm is put in a zone of silence[3] after the nozzle to achieve a well localized supersonic gas-jet with a small transversal momentum to the direction of the gas-jet, meanwhile not to break down the ultrahigh vacuum state of the reaction chamber. The transmitted internally cold gas target then passes through a small aperture with a size of ~1.0 mm into the reaction chamber. The usage of the aperture is for the gas beam collimation. A second aperture was also applied for further collimation, as shown in Fig.4[34].

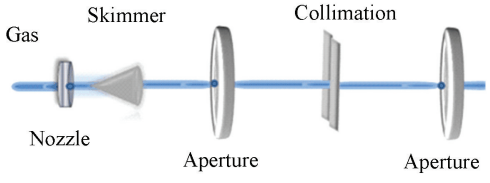

Fig.4 The gas-jet target with two apertures in the COLTRIMS apparatus[34]

Increasing the number of the skimmers in COLTRIMS also helps lower the uncertainty of thermal momentum of gas-jet targets. Two skimmers have been used experimentally to reduce the gas-jet diameter at the interaction region[35-36]. The second skimmer lowers the momentum uncertainty perpendicular to the direction of the beam propagation and decreases the spatial target extension of the sample in this direction. The use of the two skimmers can also minimize the uncertainty of thermal momentum of the molecular gas-jet in the direction perpendicular to its propagation.

For atomic gas-jet target, the combined setup of a magneto-optical trap (MOT) with a reaction microscope has been designed for investigating atomic break-up processes in a kinematically complete way[37]. The MOT pre-cools atoms and allows for the performance at a typical much lower temperature of <1 mK. With this novel combination, the momentum vectors of the produced lithium ions were measured in coincidence over the full solid angle. The achieved momentum resolution was excellent, which is comparable or little better than that in the conventional COLTRIMS measurements.

3.4 Different Designs for Electron- and Ion-Impact

When the molecular dynamics is induced by charged particle impact, the CMI system should be carefully considered to eliminate the influence of the extraction field on the incident electron or ion beam.

In the electron-impact case, a particular electron optical lens[38-39] was applied to avoid the extraction field influence. However the deviation of the electron beam was eliminated to a certain degree but could not be completely eliminated. A pulsed electric field was employed in a spectrometer recently to extract the recoil ions meanwhile to avoid the extraction field influence on the electron beam[40-41]. Furthermore, a combination of a static extraction field with deflection plates was also employed[40]. The use of the static extraction field can avoid the effect of the field switching blurring on the measured kinetic energy release to some extent that exists in the pulsed extraction case. Meanwhile the deflection plates can balance the deflection from the static extraction field, as shown in Fig. 5. The Faraday cup was used to measure the current, with which the deflection plate voltages can be adjusted to gain the maximum current and to optimize the count rate.

In a recent electron-impact experiment, single or multiple ionizations of target molecules was induced by a pulsed electron beam[41]. One advantage of using the pulsed electron beam is that the background can be

significantly reduced because the birth of ions can only be within the electron pulse duration. The other advantage is to realize the coincidence measurement by using the electron gun trigger as the start signal. In this experiment a pulsed extraction field was also applied to avoid the extraction field influence.

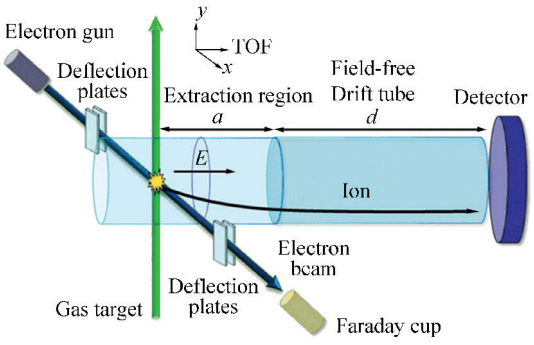

Fig.5 A pulsed extraction field combined with deflection plates used in a CMI spectrometer for electron-impact scheme[40]

In the ion-impact case, an electrostatic deflector in front of the reaction zone has been applied to separate the ion beam from charge state impurities[42-47]. An electrostatic lens was added into the spectrometer to reduce the influence of the extended interaction region on the momentum resolution of ions. Moreover, an on-axis Faraday cup was placed in front of the detector and used to collect the ion beam. It protects the detector by blocking a small portion of the signals at the center position of the imaging detector. Thus, the detector cannot detect the fragments with very low kinetic energy since they have too little transverse momentum to come out of the ion beam.

4 Application of the CMI Technique in Molecular Reaction Dynamics

In the last 20 years, due to its unique properties, the CMI technique has been extensively used to explore the reaction dynamics of molecules in various experimental conditions[9-15], which have pushed forwards current understanding on molecule behaviors in different environments. In this section we will present several representative examples of detecting molecular reaction dynamics using the CMI technique.

4.1 Coincidence Imaging of Photon-Electrons and Photon-Ions

An important application of the CMI technique is for coincidence imaging of photon-electrons and photon-ions of molecules induced by intense laser fields, from which a variety of information on ionization process and mechanism of molecules can be explored. For example, experimentally measured photo-electron spectrum can be used for extracting the structure information of molecules. Here we will present two typical examples.

By using the photon-electron photon-ion coincidence momentum imaging (PEPICO-MI), single ionization of oxygen molecules was investigated[49]. Fig. 6(a) describes the coincidence momentum imaging of O_2^+ ions and photon-electrons. Furthermore two dimensional momentum distributions of photon-electrons from single ionization of oxygen molecules were obtained, as shown in Fig.6(b), in which some typical radial structures imply the above threshold ionization mechanism.

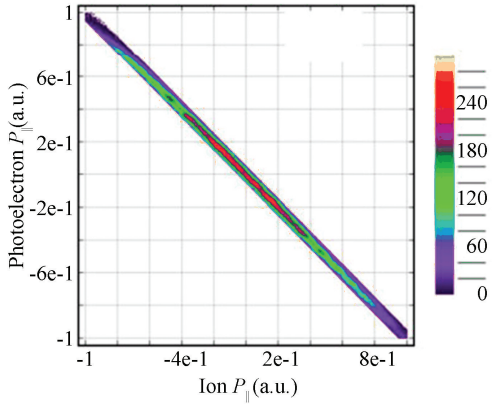

(a) Coincidence momentum map of O_2^+ ions and photon-electrons

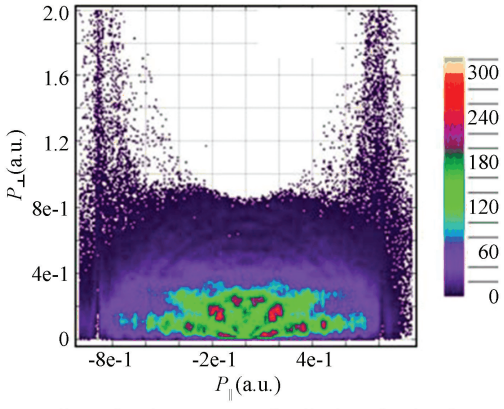

(b) Two dimensional momentum distributions for the photon-electrons produced in the single ionization of O_2 molecules by 800 nm, 24 fs laser pulses at an intensity of ~ 2×10^{14} W/cm^2

Fig.6 Coincidence momentum map of O_2^+ ions and photon-electrons, and two dimensional momentum distributions for the photon-electrons produced in the single ionization of O_2 molecules by 800 nm, 24 fs laser pulses at an intensity of ~ 2×10^{14} W/cm^2[49]

Dissociative ionization of CH_3OH in strong laser fields was also studied via PEPICO-MI method[50]. The photon-electron energy spectrum was directly measured in coincidence with the formation of CH_3OH^+, CH_2OH^+ and CH_3^+ ions, as shown in Fig. 7, from which the ionization and dissociation pathways of CH_3OH molecules could be confirmed. Moreover the peaks in each panel can help analyze the multi-photon ionization mechanism for each pathway in detail.

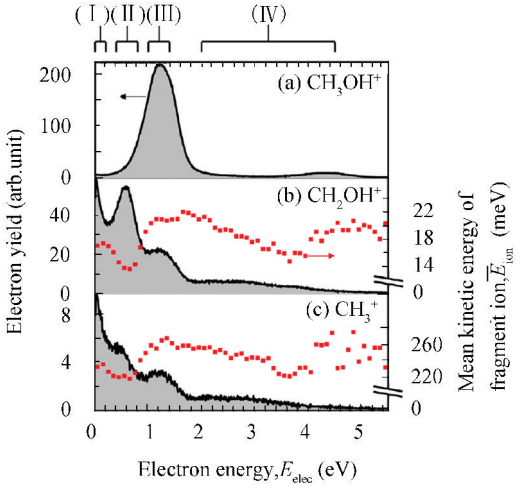

Fig. 7 The detected photon-electron energy spectrum with the coincident three ions: CH_3OH^+, CH_2OH^+ and CH_3^+ produced by strong laser fields with parameters of 398 nm, 76 fs, 8.9×10^{12} W/cm^2[50]

4.2 Identification of Coulomb Explosion Pathways

To identify a specific fragmentation pathway of a molecule from the multi-body Coulomb explosion by the CMI technique, the momentum of electrons can be neglected because the momentum imposed on an emitted electron is more than two orders of magnitude smaller than that of the fragment ions. Here we will introduce three typical applications of the CMI technique for identifying molecular Coulomb explosion pathways induced by intense laser fields, as well as by ion-impact and electron-impact by only recording the fragmented ions in the CMI measurements.

The first example is the Coulomb explosion of O_2 molecules induced by intense femtosecond laser fields[49]. Various Coulomb explosion pathways $O_2^{(n+m)+} \rightarrow O^{n+} + O^{m+}$ were precisely identified, as shown in Fig. 8(a), in which the 3D momentum vectors with high resolution were accurately acquired from the correlated products, each island (n, m) represents the explosion pathway $O_2^{(n+m)+} \rightarrow O^{n+} + O^{m+}$. According to the obtained momentum information, the kinetic energy released from each explosion pathway can be determined, as shown in Fig.8(b). In Fig.8(b), the yields for (1, 2) and (2, 2) channels are magnified by 20 and 200 for visual convenience respectively[49].

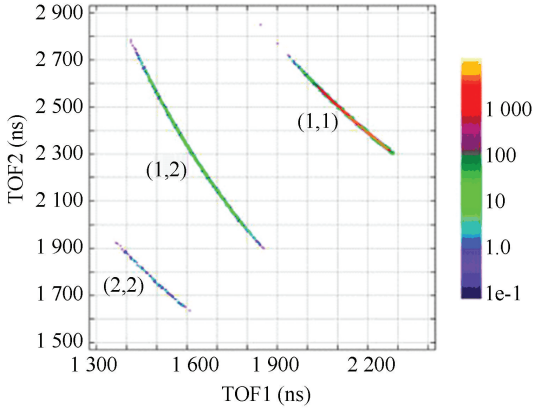

(a) Coincidence time-of-flight map of ions produced in the interaction of O_2 and 800 nm, 8 fs laser pulses at an intensity of 6×10^{14} W/cm^2

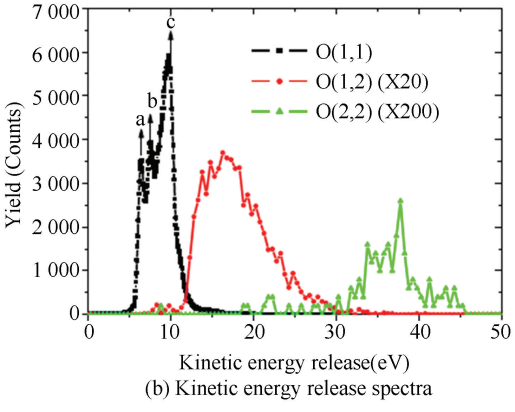

(b) Kinetic energy release spectra

Fig. 8 Coincidence time-of-flight map of ions produced in the interaction of O_2 and 800 nm, 8 fs laser pulses at an intensity of 6×10^{14} W/cm^2, and kinetic energy release spectra

The second example is the investigation of Coulomb explosion of OCS molecules which was produced by impact of 15 keV/q Ar^{4+} and Ar^{8+} ions[51]. Several fragmentation pathways from (1,1,1) to (2,2,2), where (a,b,c) corresponds to the production of fragments $O^{a+} + C^{b+} + S^{c+}$, could be accessed via changing the projectile ion. Moreover whether the pathways were concerted or stepwise was successfully identified as well.

The third example is the demonstration of the

momentum spectroscopy of recoil ions from a multiply charged N_2O molecule by impact of 10 keV electrons[52]. The Coulomb explosion pathways for N_2O^{2+} and N_2O^{3+} ions in both complete and incomplete manners were determined from the CMI measurements. Meanwhile whether the fragmentation pathways were concerted or sequential was also examined.

4.3 Determination of Molecular Isomers

The determination of molecular isomers especially chiral molecules has recently attracted much attention. It was a long-term challenge to identify the absolute configuration of chiral molecules in gas phase. In the year 2013, with the CMI technique, direct demonstration of the absolute configuration of individual molecules was successfully obtained by measuring laser-induced Coulomb explosion of the chiral molecule CHBrClF in gas phase[53]. The measured result, as shown in Fig. 9, was a clear evidence for the absolute configuration of the enantiomers.

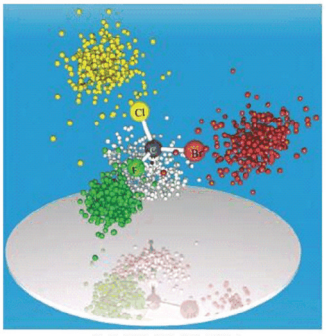

(a) (S)-CHBrClF

(b) (R)-CHBrClF

Fig. 9 Measured linear momenta in fivefold fragmentation of CHBrClF enantiomers. The color codes correspond to: C, gray arrow; H, white; F, green; Cl, yellow; Br, red[53]

In the same year, the determination of molecular isomers was also demonstrated experimentally by imaging foil-induced Coulomb explosion of isotopically labeled (*R*,*R*)-2,3-dideuterooxirane chiral molecule in gas phase using the CMI technique[54]. The measured results show an obvious difference in the absolute configuration of racemic oxirane and enantiopure oxirane.

Furthermore, with the CMI technique, photoelectron circular dichroism of chiral molecule methyloxirane enantiomers induced by a 420-nm femtosecond laser pulse was observed as a result of a asymmetry in the angular distribution of photoelectrons[55], from which the chiral terms could be isolated by comparing the difference of the full 3D electron momentum distributions measured with the conditions of left- and right-circular polarizations. Moreover, the decomposition process of two isomers 2,6- and 3,5-difluoroiodobenzene induced by soft X-rays were also investigated by using the CMI technique[56]. The two isomers were experimentally distinguished by examining the momentum correlation maps of fluorine and iodine cations in triple-ion coincidence measurement.

4.4 Enhanced Ionization

The CMI technique was recently used to investigate a so-called enhanced ionization phenomenon of molecules, in which the ionization occurs at a critical internuclear distance R_c, where the ionization rate of molecules is significantly enhanced than that in the case of either the equilibrium internuclear distance or a much longer internuclear distance. The yield of multiply charged fragmenting ethylene and acetylene molecules induced by the laser fields with different laser intensities and pulse durations was measured[57], as shown in Fig. 10. A significant increase of the H^+ energy was observed when the laser pulse duration increased while the laser intensity was kept to be constant. This reveals that longer pulse duration leads to a strong enhancement in the yield of highly-charged parent molecular ions. The enhancement was ascribed to the resultant higher population of the precursor states that favors fast C-H stretch at R_c, where enhanced ionization occurs. The increase of the pulse duration leads to these precursor states to be more efficiently populated, resulting in the larger probability of the enhanced ionization. This study experimentally confirmed the existence of enhanced ionization in hydrocarbon molecules.

4.5 Dissociative Ionization Cross Sections

Recently the CMI technique has also been applied

for investigating dissociative ionization cross sections of molecules. The kinetic energy distribution and the relative cross section of CH_4 induced by electron impact were experimentally studied[40]. The ratio of the produced dissociative CH_n^+ ($n = 0 \sim 3$) ions to the CH_4^+ ions was measured with incident electron energy of 20−200 eV. The distribution of the kinetic energy of the ions was shown and the average KER of CH_3^+ was obtained.

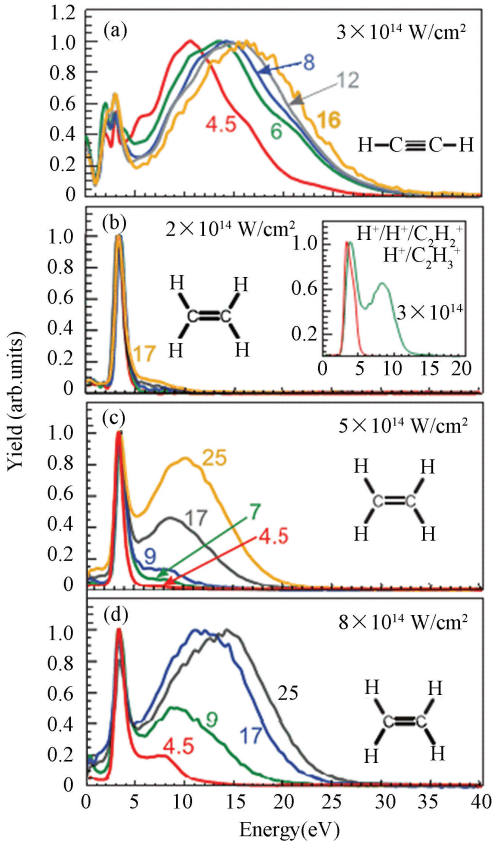

Fig.10 Measured energy spectra of protons ejected from acetylene (a) and ethylene [(b)-(d)] induced by the laser pulses with different intensities and durations[57]

By using the CMI technique the cross section of dissociative ionization of carbon dioxide CO_2 molecules by electron impact with an energy of 5 keV were investigated[58]. The two-body and three-body fragmentation pathways of CO_2^{2+} and CO_2^{3+} were determined and the cross sections of the partial ionization of different fragments were obtained.

Moreover the investigation of quadruple differential dissociative ionization cross sections of of H_2 by electron-impact was also reported[59]. The H_2 molecule was ionized and the H_2^+ ion was simultaneously excited with immediate dissociation. Results from theoretical molecular four-body distorted wave calculations match experimental data well.

4.6 Control of Molecular Reaction Dynamics

The CMI technique has also been applied for probing molecular reaction processes manipulated by different experimental conditions, such as pulse width[60], wavelength[34], intensity[61], polarization state[61], and shape of the laser pulses[62]. In the following we will present three experimental observations, i. e., molecular pathway interference, chemical bond breaking and ultrafast proton migration by using the CMI technique.

Control of the pathway interference in dissociation of H_2^+ ions by the carrier envelope phase (CEP) of short intense fields was recently demonstrated by using the 3D CMI technique[46]. The emission direction of fragmented H^+ ions relative to the laser polarization showed CEP-dependent asymmetries, which were attributed to the interference of even and odd photon number pathways. It was verified that the interference of net zero-photon and one-photon contributes at the $H^+ + H$ KERs in the range of 0.2−0.45 eV, and that of the net two-photon and one-photon contributes the KERs in the range of 1.65−1.9 eV.

Manipulation of chemical bond breaking was also demonstrated recently[63-64]. The CEP dependence in the C-D bond breaking of C_2D_2 induced by a strong few-cycle pulse was investigated experimentally by the CMI technique[63]. The CEP-dependent asymmetry in the ejection direction of D^+ from the Coulomb explosion, $C_2D_2^{2+} \rightarrow C_2D^+ + D^+$, was observed. The CEP dependence is exhibited to be out of phase by π with respect to that of $C_2D_2^+$. Selective bond breaking of CO_2 induced by phase-locked dual-color strong laser pulses was investigated by the CMI technique[64]. The asymmetric distributions along the direction of the laser polarization was demonstrated for the fragment ions CO^+ and O^+ generated by the Coulomb explosion, $CO_2^{2+} \rightarrow O^+ + CO^+$. This reflected the fact that although the two C-O bonds were equivalent, one of them was selectively broken by the two-color laser fields. It was also demonstrated that the largest asymmetry takes place at lower field intensities.

Control of ultrafast proton migration in CH_3Cl molecules by strong laser pulses at two different laser frequencies was also investigated by the CMI technique[34]. From the measured kinetic energy release distributions, the H^+ migration in different

charged parent molecules was investigated. Selective control of H^+ migration in CH_3Cl molecules was realized by controlling different fragmentation pathways using different laser frequencies, as shown in Fig.11.

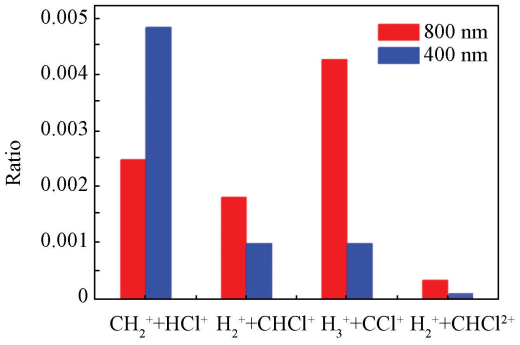

Fig. 11 The relative yield ratios of different fragmentation pathways at different laser wavelengths. Red: 800 nm laser field; blue: 400 nm laser field[34]

4.7 Time-Resolved Molecular Reaction Dynamics

Visualizing ultrafast molecular reaction dynamics in real time is a very attractive topic. Probing complex dynamics using time-resolved multi-dimensional CMI of 1,3-butadiene with 200-nm laser pulses has been implemented experimentally[65]. Complex temporal behaviors were observed in time-resolved angular distribution of photoelectrons that are sensitive to the dynamics, and also include rich information that makes understanding of these complex dynamics difficult.

Using a pair of strong ultrashort laser pulses, time-resolved probing of Coulomb explosion of CS_2 in highly charged states by the CMI technique was reported[66]. It was shown that the time scale of the Coulomb explosion proceeding of CS_2 is strongly dependent on the charged states, and the explosion the two CS bonds is mainly along the linear geometry.

Time-resolved investigations of molecules in gas phase with free electron lasers using the CMI technique were also reported[67]. A Nd: YAG laser pulse at 1064 nm was used to adiabatically align the 1-ethynyl-4-fluorobenzene (C_8H_5F, pFAB) molecules, and a second femtosecond laser pulse from a Ti: Sapphire laser (266/400/800 nm) was used to initiate a photochemical reaction of the aligned molecule. A third femtosecond X-ray pulse from a free electron laser was employed to subsequently probe the reaction at various time-delays via photoelectron diffraction. Using the CMI technique, the VMI images of the fragmented F^+ ions and the angular distributions of F(1s) photoelectrons generated from the photoionization of the laser-aligned pFAB molecules were obtained.

Based on the KER distributions of the fragments ejected respectively from the $CH_3OH^{2+} \rightarrow CH_2^+ + OH_2^+$ and $CH_3OH^{2+} \rightarrow CH_3^+ + OH^+$ pathways, ultrafast nuclear dynamics of CH_3OH^+ induced by few-cycle pulses was investigated using the pump-probe CMI technique[68]. As shown in Fig. 12, an oscillation in the measured KER distribution was observed for the migration pathway, which shows a bifurcation structure at ~150 fs. This observation was explained as follows. A vibrational wave packet is prepared on a bound well around the migrated geometry, which first oscillates along the C-O bond, and then bifurcates into the bound well and the dissociating potential curves.

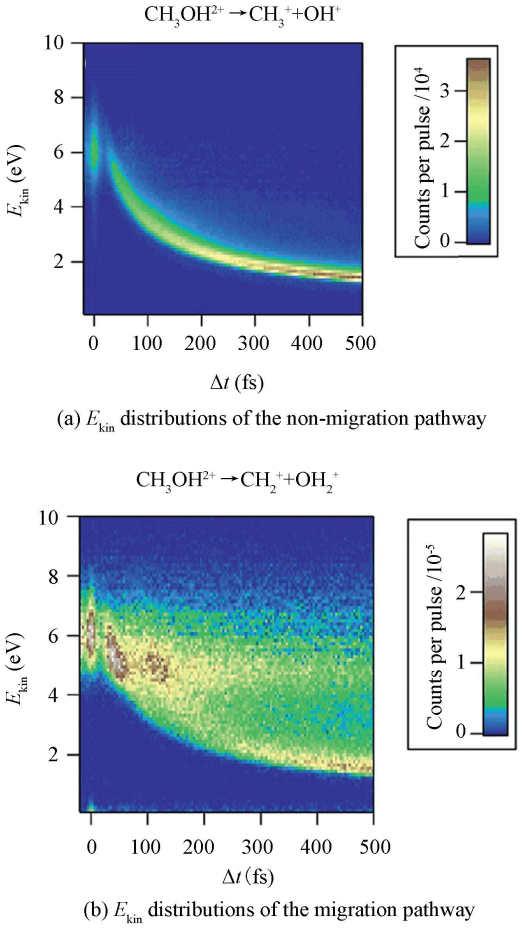

Fig.12 E_{kin} distributions of the non-migration and migration pathway with pump-probe time delay Δt[68]

5 Summary

In this article, we present an overview of recent progress in the CMI technique. We first gave an introduction to how the CMI technique can work for detecting 3D momentum vectors of photon-ions and photon-electrons ejected from a single parent molecule, and thus enabling the reconstruction of molecular electronic and geometrical structures. We then discussed the advantages of different CMI designs with different device components including spectrometer, detector, and gas-jet target, which are generally required to be modified accordingly based on the employed excitation sources, such as intense laser pulses, ion- and electron-impact. Lastly, application examples of the CMI technique in molecular reaction dynamics such as identifying molecular Coulomb explosion pathways, determination of molecular isomers, investigating ionization dynamics including enhanced ionization and ionization cross section, control and time-resolved molecular reaction dynamics were presented, which demonstrated the powerful capabilities of the CMI technique in studying molecular reaction dynamics.

Despite the CMI technique has many advantages in studying molecular reaction dynamics, it has also some drawbacks. Firstly, it is usually destructive because neutral molecular structure is destroyed during ionization or fragmentation for subsequent detection. Secondly, the application of this technique is normally restricted to an isolated molecular system in gas phase, and nowadays it is still limited in application to condensed-phase molecules. Lastly, the CMI technique needs a light source with high repetition rate for a reasonable data acquisition time.

We also noticed that a novel nondestructive scheme was recently developed. With strong pump pulse stimulated Raman scattering is induced to monitor structural deformations and relaxations of liquid molecules in real time[69]. Moreover a new technique called femtosecond time-resolved transient grating technique, provides an effective way for investigating photodissociation mechanism in liquid molecules[70]. These new techniques have pushed forward studies of molecular dynamics of materials in liquid phase.

We expect that this article can provide readers a fundamental and detailed insight into the CMI technique and thus help them make full use of the unique characteristics of the CMI technique in their research areas. We expect that with the rapid progress of laser technologies the CMI technique will be applied in many different research fields with the matters in all the gas, liquid and solid phases. We also expect possible combination of the powerful CMI tool with other advanced techniques for providing great abilities in as many as scientific study prospects, for example a combination of attosecond pulses with COLTRIMS, so called AttoCOLTRIMS, for attosecond science[71].

References

[1] Hasegawa H, Hishikawa A, Yamanouchi K. Coincidence imaging of Coulomb explosion of CS_2 in intense laser fields. Chemical Physics Letters, 2001, 349(1-2): 57-63. DOI: 10.1016/S0009-2614(01)01087-9.

[2] Ullrich J, Moshammer R, Dörner R, et al. Recoil-ion momentum spectroscopy. Journal of Physics B: Atomic, Molecular and Optical Physics, 1997, 30(13): 2917-2974. DOI: 10.1088/0953-4075/30/13/006.

[3] Dörner R, Mergel V, Jagutzki O, et al. Cold target recoil ion momentum spectroscopy: a ´momentum microscope´ to view atomic collision dynamics. Physics Reports, 2000, 330(2-3): 95-192. DOI: 10.1016/S0370-1573(99)00109-X.

[4] Ullrich J, Moshammer R, Dorn A, et al. Recoil-ion and electron momentum spectroscopy: reaction-microscopes. Reports on Progress in Physics, 2003, 66(9): 1463-1545. DOI: 10.1088/0034-4885/66/9/203.

[5] Eppink A, Parker D. Velocity map imaging of ions and electrons using electrostatic lenses: Application in photoelectron and photofragment ion imaging of molecular oxygen. Review of Scientific Instruments, 1997, 68(9): 3477-3484. DOI: 10.1063/1.1148310.

[6] Xu Huailiang, Okino T, Nakai K, et al. Hydrogen migration and C-C bond breaking in 1, 3-butadiene in intense laser fields studied by coincidence momentum imaging. Chemical Physics Letters, 2010, 484(4-6): 119-123. DOI: 10.1016/j.cplett.2009.11.008.

[7] Waitz M, Bello R Y, Metz D, et al. Imaging the square of the correlated two-electron wave function of a hydrogen molecule. Nature Communications, 2017, 8: 2266. DOI: 10.1038/s41467-017-02437-9.

[8] Kling M F, Siedschlag Ch, Verhoef A J, et al. Control of electron localization in molecular dissociation. Science, 2006, 312(5771): 246-248. DOI: 10.1126/science.1126259.

[9] Moshammer R, Feuerstein B, Schmitt W, et al. Momentum distributions of Ne^{n+} ions created by an intense ultrashort laser pulse. Physical Review Letters, 2000, 84(3): 447-450. DOI: 10.1103/PhysRevLett.84.447.

[10] Fischer A, Sperl A, Cörlin P, et al. Electron Localization Involving Doubly Excited States in Broadband Extreme Ultraviolet Ionization of H_2. Physical Review Letters, 2013, 110(21): 213002. DOI: 10.1103/PhysRevLett.110.213002.

[11] Dorn A, Moshammer R, Schröter C D, et al. Double ionization of helium by fast electron impact. Physical Review Letters, 1999, 82(12), 2496-2499. DOI: 10.1103/PhysRevLett.82.2496.

[12] Schulz M, Moshammer R, Fischer D, et al. Three-dimensional imaging of atomic four-body processes. Nature, 2003, 422(6927): 48-50. DOI: 10.1038/nature01415.

[13] Oghbaie S, Gisselbrecht M, Laksman J, et al. Dissociative double-photoionization of butadiene in the 25-45 eV energy range using 3-D multi-coincidence ion momentum imaging spectrometry. The Journal of Chemical Physics, 2015, 143(11): 114309. DOI: 10.1063/1.4931104.

[14] Weber T, Czasch A O, Jagutzki O, et al. Complete photo-fragmentation of the deuterium molecule. Nature, 2004, 431(7007): 437-440. DOI: 10.1038/nature02839.

[15] Moshammer R, Jiang Yuhai, Foucar L, et al. Few-photon multiple ionization of Ne and Ar by strong free-electron-laser pulses. Physical Review Letters, 2007, 98(20): 203001. DOI: 10.1103/PhysRevLett.98.203001.

[16] Kanya R, Kudou T, Schirmel N, et al. Hydrogen scrambling in ethane induced by intense laser fields: Statistical analysis of coincidence events. The Journal of Chemical Physics, 2012, 136(20): 204309. DOI: 10.1063/1.4720503.

[17] Graham L, Zohrabi M, Gaire B, et al. Fragmentation of CD^+ induced by intense ultrashort laser pulses. Physical Review A, 2015, 91(2): 023414. DOI: 10.1103/PhysRevA.91.023414.

[18] Pitzer M, Kastirke G, Burzynski P, et al. Stereochemical configuration and selective excitation of the chiral molecule halothane. Journal of Physics B: Atomic, Molecular and Optical Physics, 2016, 49(23): 234001. DOI: 10.1088/0953-4075/49/23/234001.

[19] Keller H, Klingelhöfer G, Kankeleit E. A position sensitive microchannel plate detector using a delay line readout anode. Nuclear Instruments & Methods in Physics Research Section A: Accelerators, Spectrometers, Detectors and Associated Equipment, 1987, 258: 221-224.

[20] Becker J, Beckord K, Werner U, et al. A system for correlated fragment detection in dissociation experiments. Nuclear Instruments & Methods in Physics Research Section A: Accelerators, Spectrometers, Detectors and Associated Equipment, 1994, 337: 409-415.

[21] Jagutzki O, Lapington J S, Worth L B C, et al. Position sensitive anodes for MCP read-out using induced charge measurement. Nuclear Instruments & Methods in Physics Research Section A: Accelerators, Spectrometers, Detectors and Associated Equipment, 2002, 477: 256-261.

[22] Martin C, Jelinsky P, Lampton M, et al. Wedge-and-strip anodes for centroid-finding position-sensitive photon and particle detectors. Review of Scientific Instruments, 1981, 52(7): 1067-1074. DOI: 10.1063/1.1136710.

[23] Strasser D, Urbain X, Pedersen H B, et al. An innovative approach to multiparticle three-dimensional imaging. Review of Scientific Instruments, 2000, 71(8): 3092-3098. DOI: 10.1063/1.1305514.

[24] Chichinin A I, Gericke K H, Kauczok S, et al. Imaging chemical reactions-3D velocity mapping. International Reviews in Physical Chemistry, 2009, 28(4): 607-680. DOI: 10.1080/01442350903235045.

[25] Slater C S, Blake S, Brouard M, et al. Covariance imaging experiments using a pixel-imaging mass-spectrometry camera. Physical Review A, 2014, 89(1): 011401(R). DOI: 10.1103/PhysRevA.89.011401.

[26] Long Jingming, Furch F J, Durá J, et al. Ion-ion coincidence imaging at high event rate using an in-vacuum pixel detector. The Journal of Chemical Physics, 2017, 147(1): 013919. DOI: 10.1063/1.4981126.

[27] Lee S K, Cudry F, Lin Yunfei, et al. Coincidence ion imaging with a fast frame camera. Review of Scientific Instruments, 2014, 85(12): 123303. DOI: 10.1063/1.4903856.

[28] Fan Lin, Lee S K, Tu Yi-Jung, et al. A new electron-ion coincidence 3D momentum-imaging method and its application in probing strong field dynamics of 2-phenylethyl-*N*, *N*-dimethylamine. The Journal of Chemical Physics, 2017, 147(1): 013920. DOI: 10.1063/1.4981526.

[29] Hanold K A, Luong A K, Clements T G, et al. Photoelectron-multiple-photofragment coincidence spectrometer. Review of Scientific Instruments, 1999, 70(5): 2268-2276. DOI: 10.1063/1.1149751.

[30] Jagutzki O, Cerezo A, Czasch A, et al. Multiple hit read-out of a microchannel plate detector with a three-layer delay-line anode. 2001 IEEE Nuclear Science Symposium Conference Record, 2002, 1-4: 850-854. DOI: 10.1109/NSSMIC.2001.1009689.

[31] Da Costa G, Vurpillot F, Bostel A, et al. Design of a delay-line position-sensitive detector with improved performance. Review of Scientific Instruments, 2005, 76(1): 013304. DOI: 10.1063/1.1829975.

[32] Wallauer R, Voss S, Foucar L, et al. Momentum spectrometer for electron-electron coincidence studies on superconductors. Review of Scientific Instruments, 2012, 83(10): 103905. DOI: 10.1063/1.4754470.

[33] Jagutzki O, Cerezo A, Czasch A, et al. Multiple hit readout of a microchannel plate detector with a three-layer delay-line anode. IEEE Transactions on Nuclear Science, 2002, 49(5): 2477-2483. DOI: 10.1109/TNS.2002.803889.

[34] Ma Pan, Wang Chuncheng, Li Xiaokai, et al. Ultrafast

proton migration and Coulomb explosion of methyl chloride in intense laser fields. The Journal of Chemical Physics, 2017, 146(24): 244305. DOI: 10.1063/1.4989565.

[35] Kim H-K, Gassert H, Schöffler M S, et al. Ion-impact-induced interatomic Coulombic decay in neon and argon dimers. Physical Review A, 2013, 88(4): 042707. DOI: 10.1103/PhysRevA.88.042707.

[36] Sturm F P, Wright T W, Ray D, et al. Time resolved 3D momentum imaging of ultrafast dynamics by coherent VUV-XUV radiation. Review of Scientific Instruments, 2016, 87(6): 063110. DOI:10.1063/1.4953441.

[37] Hubele R, Schuricke M, Goullon J, et al. Electron and recoil ion momentum imaging with a magneto-optically trapped target. Review of Scientific Instruments, 2015, 86(3): 033105. DOI:10.1063/1.4914040.

[38] Sharma V, Bapat B. An apparatus for studying momentum-resolved electron-impact dissociative and non-dissociative ionisation. The European Physical Journal D-Atomic, Molecular, Optical and Plasma Physics, 2006, 37(2): 223-229. DOI: 10.1140/epjd/e2005-00267-5.

[39] Singh R, Bhatt P, Yadav N, et al. Momentum mapping spectrometer for probing the fragmentation dynamics of molecules induced by keV electrons. Measurement Science and Technology, 2011, 22(5): 055901. DOI: 10.1088/0957- 0233/22/5/055901.

[40] Wei B, Chen Z, Wang X, et al. The relative cross section and kinetic energy distribution of dissociation processes of methane by electron impact. Journal of Physics B: Atomic, Molecular and Optical Physics, 2013, 46(21): 215205. DOI: 10.1088/0953-4075/46/21/215205.

[41] Wang Enliang, Shan Xu, Shi Yufeng, et al. Momentum imaging spectrometer for molecular fragmentation dynamics induced by pulsed electron beam. Review of Scientific Instruments, 2013, 84(12): 123110. DOI:10.1063/ 1.4847156.

[42] Zohrabi M, McKenna J, Gaire B, et al. Vibrationally resolved structure in O_2^+ dissociation induced by intense ultrashort laser pulses. Physical Review A, 2011, 83(5): 053405. DOI:10.1103/PhysRevA.83.053405.

[43] Gaire B, McKenna J, Zohrabi M, et al. Dynamics of D_3^+ slow dissociation induced by intense ultrashort laser pulses. Physical Review A, 2012, 85(2): 023419. DOI: 10.1103/ PhysRevA.85.023419.

[44] Sayler A M, McKenna J, Gaire B, et al. Measurements of intense ultrafast laser-driven D_3^+ fragmentation dynamics. Physical Review A, 2012, 86(3): 033425. DOI:10.1103/ PhysRevA.86.033425.

[45] Kling N G, McKenna J, Sayler A M, et al. Charge asymmetric dissociation of a CO^+ molecular-ion beam induced by strong laser fields. Physical Review A, 2013, 87(1): 013418. DOI:10.1103/PhysRevA.87.013418.

[46] Kling N G, Betsch K J, Zohrabi M, et al. Carrier-envelope phase control over pathway interference in strong-field dissociation of H_2^+. Physical Review Letters, 2013, 111(16): 163004. DOI: 10.1103/PhysRevLett.111.163004.

[47] Trinter F, Waitz M, Schöffler M, et al. Search for isotope effects in projectile and target ionization in swift He^+ on H_2 or D_2 collisions. Physical Review A, 2014, 89(3): 032702. DOI:10.1103/PhysRevA.89.032702.

[48] Yang Bo-si, Zhang Li, Xu Huai-Liang, et al. Fragmentation of hydrocarbon molecules in intense laser fields studied by coincidence momentum imaging: A review. Chinese Journal of Physics, 2014, 52 (1-II): 652-674. DOI: 10.6122/CJP.52.652.

[49] Wu Cong, Wu Chengyin, Yang Yudong, et al. Coincidence imaging of photoelectrons and photo-ions of molecules in strong laser fields. Journal of Modern Optics, 2013, 60 (17): 1388-1394. DOI: 10.1080/09500340.2013.798431.

[50] Fukahori S, Nakano M, Yamanouchi K, et al. Channel-specific photoelectron angular distribution in laboratory and molecular frames for dissociative ionization of methanol in intense ultraviolet laser fields. Chemical Physics Letters, 2017, 672: 7-12. DOI: 10.1016/j.cplett.2017.01.043.

[51] Wales B, Motojima T, Matsumoto J, et al. Coincidence momentum imaging of the Coulomb explosion of OCS induced by collision of 15keV/q Ar^{4+} Ar^{8+} Ions. Journal of Physics: Conference Series, 2012, 388 (Part 10): 102057. DOI:10.1088/1742-6596/388/10/102057.

[52] Bhatt P, Singh R, Yadav N, et al. Momentum spectroscopy of fragment ions of a multiply charged N_2O molecule under impact of 10-keV electrons. Physical Review A, 2012, 86 (5): 052708. DOI: 10.1103/PhysRevA.86.052708.

[53] Pitzer M, Kunitski M, Johnson A S, et al. Direct determination of absolute molecular stereochemistry in gas phase by coulomb explosion imaging. Science, 2013, 341 (6150): 1096-1099. DOI: 10.1126/science.1240362.

[54] Herwig P, Zawatzky K, Grieser M, et al. Imaging the absolute configuration of a chiral epoxide in the gas phase. Science, 2013, 342(6162): 1084-1086. DOI: 10.1126/science.1246549.

[55] Rafiee Fanood M M, Powis I, Janssen M H M. Chiral asymmetry in the multiphoton ionization of methyloxirane using femtosecond electron-ion coincidence imaging. The Journal of Physical Chemistry A, 2014, 118 (49): 11541-11546. DOI:10.1021/jp5113125.

[56] Ablikim U, Bomme C, Savelyev E, et al. Isomer-dependent fragmentation dynamics of inner-shell photoionized difluoroiodobenzene. Physical Chemistry Chemical Physics, 2017, 19(21): 13419-13431. DOI: 10.1039/c7cp01379e.

[57] Xie Xinhua, Roither S, Schöffler M, et al. Role of proton dynamics in efficient photoionization of hydrocarbon molecules. Physical Review A, 2014, 89(2): 023429. DOI:10.1103/PhysRevA.89.023429.

[58] Wang Enliang, Shen Zhenjie, Yang Hongjiang, et al. Dissociative ionization cross sections of CO_2 at electron impact energy of 5 keV. Chinese Physics B, 2014, 23(11): 113404. DOI: 10.1088/1674-1056/23/11/113404.

[59] Ali E, Ren Xueguang, Dorn A, et al. Experimental and theoretical study of electron-impact ionization plus excitation of aligned H_2. Journal of Physics B: Atomic, Molecular and Optical Physics, 2015, 48(11): 115201. DOI:10.1088/0953-4075/48/11/115201.

[60] Yazawa H, Shioyama T, Hashimoto H, et al. Non-adiabatic transition in $C_2H_5OH^+$ on a light-dressed potential energy surface by ultrashort pump-and-probe laser pulses. Applied Physics B-Lasers and Optics, 2010, 98(2-3):275-282. DOI: 10.1007/s00340-009-3767-6.

[61] Zhang Li, Roither S, Xie X, et al. Path-selective investigation of intense laser-pulse-induced fragmentation dynamics in triply charged 1, 3-butadiene. Journal of Physics B: Atomic, Molecular and Optical Physics, 2012, 45(8): 085603. DOI: 10.1088/0953-4075/45/8/085603.

[62] Xie X, Doblhoff-Dier K, Roither S, et al. Attosecond-recollision-controlled selective fragmentation of polyatomic molecules. Physical Review Letters, 2012, 109(24): 243001. DOI: 10.1103/PhysRevLett.109.243001.

[63] Miura S, Ando T, Ootaka K, et al. Carrier-envelope-phase dependence of asymmetric C-D bond breaking in C_2D_2 in an intense few-cycle laser field. Chemical Physics Letters, 2014, 595-596: 61-66. DOI: 10.1016/j.cplett.2014.01.045.

[64] Endo T, Fujise H, Kawachi Y, et al. Selective bond breaking of CO_2 in phase-locked two-color intense laser fields: laser field intensity dependence. Physical Chemistry Chemical Physics, 2017, 19(5): 3550-3556. DOI: 10.1039/c6cp07471e.

[65] Hockett P, Ripani E, Rytwinski A, et al. Probing ultrafast dynamics with time-resolved multi-dimensional coincidence imaging: Butadiene. Journal of Modern Optics, 2013, 60(17): 1409-1425. DOI: 10.1080/09500340.2013.801525.

[66] Matsuda A, Takahashi E J, Hishikawa A. Time-resolved laser Coulomb explosion imaging using few-cycle intense laser pulses: Application to exploding CS_2 in highly charged states. Journal of Electron Spectroscopy and Related Phenomena, 2014, 195: 327-331. DOI: 10.1016/j.elspec.2013.12.011.

[67] Rudenko A, Rolles D. Time-resolved studies with FELs. Journal of Electron Spectroscopy and Related Phenomena, 2015, 204(Part B): 228-236. DOI: 10.1016/j.elspec.2015.07.010.

[68] Ando T, Shimamoto A, Miura S, et al. Wave packet bifurcation in ultrafast hydrogen migration in CH_3OH^+ by pump-probe coincidence momentum imaging with few-cycle laser pulses. Chemical Physics Letters, 2015, 624: 78-82. DOI:10.1016/j.cplett.2015.02.017.

[69] Wang Y, Liu W L, Song Y F, et al. Communication: Tracking molecular structure deformation and relaxation in real time. The Journal of Chemical Physics, 2015, 143(5): 051101. DOI: 10.1063/1.4927918.

[70] Wu Honglin, Song Yunfei, Yu Guoyang, et al. Tracking the photodissociation dynamics of liquid nitromethane at 266 nm by femtosecond time-resolved broadband transient grating spectroscopy. Chemical Physics Letters, 2016, 652: 152-156. DOI: 10.1016/j.cplett.2016.04.048.

[71] Sabbar M, Heuser S, Boge R, et al. Combining attosecond XUV pulses with coincidence spectroscopy. Review of Scientific Instruments, 2014, 85(10): 103113. DOI: 10.1063/1.4898017.